Photoabsorption profile and satellite features of the potassium $4s \rightarrow 4p$ transition perturbed by ground-state helium atoms

H. Boutarfa,[1] K. Alioua,[2,3] M. Bouledroua,[3] A.-R. Allouche,[4] and M. Aubert-Frécon[4]

[1]*Physics Department, Badji Mokhtar University, B.P. 12 Annaba, Algeria*

[2]*Chérif Messadia University, B.P. 1553, Souk-Ahras 41000, Algeria*

[3]*Laboratoire de Physique des Rayonnements, Badji Mokhtar University, B.P. 12, Annaba 23000, Algeria*

[4]*Université Lyon 1, CNRS, LASIM UMR5579, bât. A. Kastler, 43 Bd du 11 novembre 1918, F-69622 Villeurbanne, France*

(Received 21 September 2012; published 8 November 2012)

Quantal calculations are performed to determine the absorption profile of the broadened potassium resonance line $4p \leftarrow 4s$ in its far wings provoked by helium perturbers. First, the $X\,^2\Sigma^+$, $A\,^2\Pi$, and $B\,^2\Sigma^+$ potentials, as well as the transition dipole moments, are carefully computed through *ab initio* methods, based on state-averaged complete active space self-consistent field multireference configuration interaction (SA-CASSCF-MRCI) calculations involving the Davidson and basis-set superposition error (BSSE) corrections. The data are then used to generate the KHe photoabsorption spectra and to examine their behavior with temperature. The theoretical profile is dominated by the *free-free* transitions and exhibits, in the vicinity of the wavelength position of 693 nm, a satellite peak in the blue wing attributed to the $B \leftarrow X$ transitions. The results are compared with previous theoretical and experimental investigations and, in general, good agreement is found.

DOI: 10.1103/PhysRevA.86.052504 PACS number(s): 32.70.Jz, 32.80.−t, 31.50.Bc, 31.50.Df

I. INTRODUCTION

The study of the alkali-metal–rare-gas systems has in recent years become a subject of great importance in various fields of fundamental and applied physics, such as in astrophysics, quantum chemistry, and laser physics, to name just a few. This is particularly due to the presence of repulsive ground states, to the stability of their first-excited states, and to the occurrence of broad-resonance-line blue satellites.

Indeed, a few number of theoretical investigations [1–7] and experimental measurements [8–10] have been lately interested in determining the pressure-broadened profile of alkali metals perturbed by rare gases using different methods. Exploring the photoabsorption spectra of the alkali-metal–rare-gas systems and locating the possible satellite peaks allow us to study the physical and chemical properties of the atmospheres of brown dwarfs and extrasolar giant planets dominated by alkali-metal atoms. The obtained spectra may therefore constitute strong tools for understanding such astrophysical objects [11–14]. The analysis of the alkali-metal–rare-gas systems is additionally aimed at revealing some interesting features used in manufacturing high-quality exciplex lasers, based on the dissociation of the moderately stable first-excited state into the repulsive ground state [15,16]. It can further predict the construction of a newly emerged class of photoassociation lasers, based on the photoexcitation of the resonance-line blue satellite and alkali-metal–rare-gas excimer dissociation [17,18]. Such lasers can be designed for a wide range of medical, industrial, and military applications.

In this paper, our attention is more focused on the *quantal* evaluation of the far-wing pressure broadening parameters by considering the low-density limit, in connection with the potassium K($4p \leftarrow 4s$) resonance line perturbed by ground helium He($1s^2$) atoms. For this purpose, we have chosen to use the potential-energy curves and transition dipole moments of the KHe molecule which we have generated by *ab initio* calculations, where we adopted the state-averaged complete active space self-consistent field (SA-CASSCF) with the multireference configuration interaction (MRCI) methods. The accuracy of the ground $X\,^2\Sigma^+$ and excited $A\,^2\Pi$ and $B\,^2\Sigma^+$ states, with the corresponding $D_{\Sigma\text{-}\Pi}$ and $D_{\Sigma\text{-}\Sigma}$ transition moments, is examined at different temperatures by calculating the diffusion coefficients of the $4s$ or $4p$ potassium atom moving in a helium gas and the lifetimes of the levels of the $A\,^2\Pi$ state. We then investigate the shape and intensity of the photoabsorption spectra at various temperatures and determine the position of the eventual satellites in the wings and specify the type and origin of the radiative transitions from which the satellites may arise. Finally, we compare the calculated pressure-broadening profiles with other theoretical studies performed by Allard *et al.* [1] and Zhu *et al.* [5] and also with experimental data measured by Shindo and Yoshino [19,20].

Unless otherwise stated, most of the data given below are in atomic units (a.u.).

II. REDUCED ABSORPTION COEFFICIENTS

The broadened $4p \leftarrow 4s$ atomic photoabsorption line of potassium by helium is attributed to transitions from the KHe quasimolecular ground state $X\,^2\Sigma^+$ to the excited states $A\,^2\Pi$ and $B\,^2\Sigma^+$. Both X and B doublet Σ states are known to be purely repulsive, whereas the A doublet Π state forms a very shallow well; we then consider in such a case only the two *free-free* (ff) and *free-bound* (fb) transitions.

The pressure broadening of the potassium K($4p \leftarrow 4s$) resonance line, of frequency ν_0, by ground helium He($1s^2$) atoms is characterized by the quantum-mechanical *reduced* absorption coefficients k_r at frequency ν defined as the number of absorbed photons per unit volume per unit time per unit interval frequency divided by the product of the atomic number densities of potassium and helium, as adopted in our previous works [6,7]. The *free-free* reduced absorption coefficient $k_r^{ff}(\nu)$, corresponding to the transitions from all the *lower* continuum levels $(\epsilon'', J'', \Lambda'')$ to all the *upper* continuum

levels $(\epsilon', J', \Lambda')$, is given at temperature T by

$$k_r^{ff}(\nu) = \frac{8\pi^3\nu}{3c}\omega\left(\frac{2\pi\hbar^2}{\mu k_B T}\right)^{3/2}\int_0^\infty d\epsilon' \sum_J (2J+1) \times |\langle\psi_{\epsilon' J'\Lambda'}|D(R)|\psi_{\epsilon'' J''\Lambda''}\rangle|^2 \exp\left(-\frac{\epsilon''}{k_B T}\right), \quad (1)$$

where $(''$) and $('$) denote the lower and upper states, respectively, and Λ represents the projection of the electronic orbital angular momentum on the internuclear axis of the KHe system. The symbols c, $\hbar$, k_B, and μ stand for the light velocity, the reduced Plank constant, the Boltzmann's constant, and the reduced mass, respectively. The continuum electronic energy levels ϵ'' and ϵ' are linked to each other by the formula $\epsilon'' = h(\nu_0 - \nu) + \epsilon'$. The probability ω that a transition takes place towards a final state is $2/3$ for the $A\,^2\Pi$ state and $1/3$ for the $B\,^2\Sigma^+$ state. Furthermore, the *free-bound* reduced absorption coefficient $k_r^{fb}(\nu)$ derived for the transitions from all the lower continuum levels $(\epsilon'', J'', \Lambda'')$ to a set of bound levels of the upper electronic states (v', J', Λ') is expressed by

$$k_r^{fb}(\nu) = \frac{8\pi^3\nu}{3c}\omega\left(\frac{2\pi\hbar^2}{\mu k_B T}\right)^{3/2}\sum_{v' J} (2J+1) \times |\langle\psi_{v' J'\Lambda'}|D(R)|\psi_{\epsilon'' J''\Lambda''}\rangle|^2 \exp\left(-\frac{\epsilon''}{k_B T}\right), \quad (2)$$

where v is the vibrational quantum number. We should mention here that the rotational quantum numbers J involved in the computations are generally large. It is therefore reasonable to assume $J'' \simeq J' = J$.

The wave functions $\psi(R)$ of the considered states appearing in both equations (1) and (2), defined at each internuclear distance R, are solutions of the radial wave equation

$$\frac{d^2\psi(R)}{dR^2} + \frac{2\mu}{\hbar^2}\left[E - V(R) - \frac{J(J+1)\hbar^2}{2\mu R^2}\right]\psi(R) = 0. \quad (3)$$

We note that the *free* wave functions $\psi(R) = \psi_{\epsilon J\Lambda}(R)$ are *energy* normalized while the *bound* wave functions $\psi(R) = \psi_{v J\Lambda}(R)$ are rather *space* normalized. The electronic potential $V(R)$ and the energy of the relative motion E are both measured with respect to the dissociation limit, while the transition dipole moment $D(R)$ tends for large R towards its atomic value D_∞.

The photoabsorption profile is generally influenced by the interaction potentials $V(R)$ and/or by the transition dipole moments $D(R)$ which must be determined accurately.

III. POTENTIAL CURVES AND TRANSITION DIPOLE MOMENTS

With the aim of determining accurately the interatomic potential energies and the transition dipole moments involved in the interaction of a ground-state He atom with a K atom either in the ground state $4s\ ^2S$ or in the first excited state $4p\ ^2P$, we have performed MRCI calculations [21,22] using reference functions derived from the SA-CASSCF approach [23,24]. Among the 21 electrons considered for KHe, only 10 inner electrons from K were frozen in subsequent calculations, so that 11 valence electrons were explicitly treated. Active space, at long range, contains the following orbitals: 7σ corresponding to K$(3s; 3p_0; 4s; 4p_0)$, He$(1s; 2s; 2p_0)$ and 6π corresponding to K$(3p_\pm; 4p_\pm)$, He$(2p_\pm)$. These 13 active orbitals are distributed as follows among the irreducible representations a_1, b_1, b_2, and a_2 of the C_{2v} symmetry: 7 3 3 0. Davidson correction is introduced to estimate the effect of higher-order excitations [25] where the entire SA-CASSCF configuration space was used as reference. The basis-set superposition error (BSSE) has been corrected *via* the counterpoise procedure [26]. The Pople valence triple zeta plus polarization 6-311++G$(2d,2p)$ basis [27] on the K atom and the Dunning correlation consistent polarized valence quadrupole zeta cc-pVQZ basis [28] on the He atom are used. Three KHe electronic states are to be determined, namely, $X\,^2\Sigma^+$, $A\,^2\Pi$, and $B\,^2\Sigma^+$, in a large range of internuclear distances $2 \leqslant R \leqslant 47a_0$, together with the corresponding transition dipole moments. Neglecting the spin-orbit effects was justified by the temperatures considered in our photoabsorption spectra problem. All calculations were performed using the quantum-chemistry package MOLPRO [29].

The obtained data points for the $X\,^2\Sigma^+$, $A\,^2\Pi$, and $B\,^2\Sigma^+$ states are further smoothly connected to the short- and long-range forms

$$V(R) \sim \alpha \exp(-\beta R), \quad (4)$$

in the case $R \leqslant 2a_0$, and

$$V(R) \sim -\frac{C_6}{R^6} - \frac{C_8}{R^8} - \frac{C_{10}}{R^{10}}, \quad (5)$$

in the case $R \geqslant 47a_0$. In these two equations, α and β are constant parameters to be determined and C_6, C_8, and C_{10} are the usual dispersion coefficients. For the long-range construction of the three states X, A, and B, the adopted values of the dispersion coefficients C_n ($n = 6$, 8, or 10) are those calculated very recently by Mitroy and Bromley [30,31] for the ground state X and by Zhang and Mitroy [32] for the excited states A and B. All the adopted C_n data, as well as the computed parameters α and β, appearing in the short- and long-range expressions (4) and (5) of $V(R)$ are listed in Table I.

The potential-energy curves we have constructed are shown in Fig. 1. The calculations confirmed in particular that both X and B states are nearly repulsive and that the A state displays a shallow well. We have found for the Xstate a well depth $D_e = 0.45\ \text{cm}^{-1}$ occurring at the equilibrium

TABLE I. Constant parameters adopted for constructed ground and excited KHe potentials in both short- and long-range regions. All data are given in atomic units.

Molecular states	Short range		Long range		
	α	β	C_6	C_8	C_{10}
$X\,^2\Sigma^+$	21.00	1.77	39.46[a]	2623[b]	2 39 800[b]
$A\,^2\Pi$	24.15	1.83	60.85[c]	1021[c]	74 550[c]
$B\,^2\Sigma^+$	23.94	1.83	103.3[c]	25 900[c]	4 625 000[c]

[a]Reference [30].
[b]Reference [31].
[c]Reference [32].

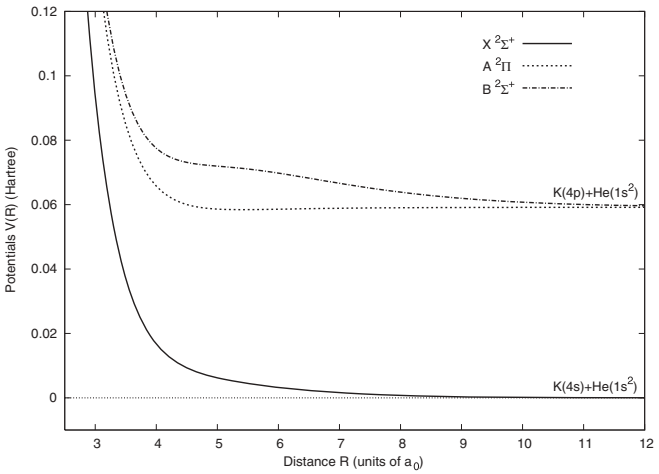

FIG. 1. Constructed KHe potentials $V(R)$ in atomic units for $X\,^2\Sigma^+$, $A\,^2\Pi$, and $B\,^2\Sigma^+$ molecular states.

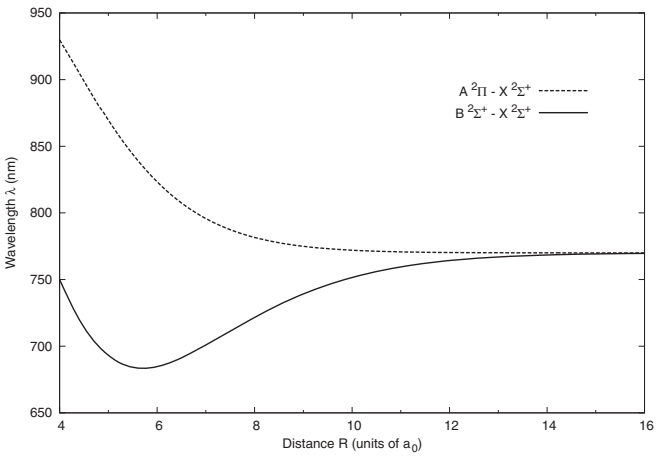

FIG. 2. Wavelengths, converted from the difference potentials for the KHe system, as a function of distance R.

position $R_e = 7.78$ Å. Nakayama and Yamashita [33], using the CASSCF-MRCI method, including the BSSE correction, have found $D_e = 0.77$ cm^{-1} and $R_e = 7.33$ Å, while Patil [34] has calculated by applying the exchange perturbation theory $D_e = 0.98$ cm^{-1} and $R_e = 7.18$ Å. Furthermore, Reho *et al.* [35] have determined in this case $D_e = 1.60$ cm^{-1} and $R_e = 7.20$ Å. One can notice that our calculated R_e value is close to those determined theoretically by these authors, while our D_e and those from Refs. [33,34] are of the same order of magnitude. The A state is found attractive with $D_e = 163$ cm^{-1} and $R_e = 2.90$ Å. Our R_e value is in good agreement with the result 2.80 Å obtained by Masnou-Seeuws *et al.* [36,37], Pascale [38], and Zbiri and Daul [39]. However, for the potential depth D_e, our result is not too far from the value $D_e = 190$ cm^{-1} of Refs. [36,37], but differs from those determined in Refs. [38] and [39] of 240 cm^{-1} and 480 cm^{-1}, respectively. For the B state, the spectroscopic data we obtained are $D_e = 0.14$ cm^{-1} and $R_e = 11.33$ Å. As far as we know, there are no data for comparison. No bound vibrational levels were obtained for the X and B states while 4 levels were obtained for the A state. The vibrational energy levels, without rotation, compared with those determined in Ref. [5] are listed in Table II, which shows a net difference between the number of levels and their respective energies. At this stage, one has to know that if we adopt the *classical* hypothesis which assumes the occurrence of absorptions from ground to excited potentials through *vertical* transitions, the satellites should appear when

TABLE II. Calculated vibrational energy levels $E(v)$ with no rotation, in cm^{-1}, for the $A\,^2\Pi$ molecular symmetry compared with those determined by Zhu *et al.* [5].

v	This work	Ref. [5]
0	−117.8	−163.7
1	−51.1	−90.45
2	−14.3	−44.82
3	−1.0	−19.11
4		−7.034
5		−1.037

the difference between the energy curves presents extrema. As illustrated in Fig. 2, we converted the difference potentials to wavelengths, in nm, and plotted them against the internuclear distance R. In particular, the potential difference $V_B - V_X$ exhibits an extremum in the vicinity of the wavelength of 683 nm which occurs near the separation $5.7a_0$. These two results are consistent with those determined with the Santra and Kirby potentials [40]; namely, 700 nm and $6.0a_0$.

The transition dipole moments $D_{\Sigma\text{-}\Pi}(R)$ and $D_{\Sigma\text{-}\Sigma}(R)$, related to the transitions from the ground X state to, respectively, the excited A and B states, have been computed by using the MRCI wave functions. We linked them to the forms $D(R) \sim D_\infty + A/R^3$, proposed by Chu and Dalgarno [41], in the large distances and $D(R) \sim a + bR$ in the short distances. Our obtained value $D_\infty = 3.07$ a.u. of the transition dipole moments, when R tends to infinity, is in good agreement with the experimental atomic value 2.92 a.u. measured by Volz and Schmoranzer [42] and Wang *et al.* [43] for the K atom. The constants $A = -4.039$, for the Σ-Π transitions, and $A = +8.618$, for the Σ-Σ transitions, are taken from Ref. [41]. Moreover, we obtained the following parameters: $a = +1.18$ and $b = +0.92$ for the Σ-Π transitions, and $a = -1.03$ and

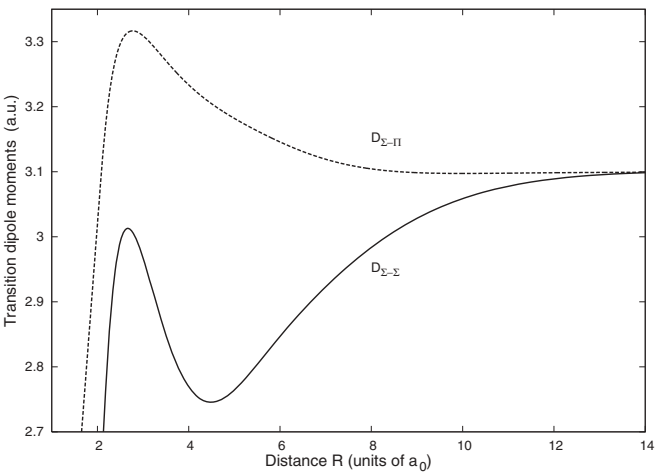

FIG. 3. Transition dipole moments $D_{\Sigma\text{-}\Sigma}(R)$ and $D_{\Sigma\text{-}\Pi}(R)$ as a function of internuclear distance R.

TABLE III. Potential energies and transition dipole moments we generated for the KHe system. Numbers in parentheses indicate powers of ten and all the data are given in a.u.

Distance	Potentials			Transition dipole moments	
R	$X\,^2\Sigma^+$	$A\,^2\Pi$	$B\,^2\Sigma^+$	$D_{\Sigma\text{-}\Pi}(R)$	$D_{\Sigma\text{-}\Sigma}(R)$
2.00	+0.6121	0.6743	0.6718	3.0187	2.4862
2.25	+0.3912			3.2136	2.8426
2.50	+0.2453	0.2955	0.2968	3.2966	2.9923
2.75	+0.1519			3.3166	3.0091
3.00	+9.3828 (−2)	0.1414	0.1471	3.3091	2.9673
3.25				3.2912	2.9074
3.50		8.4782 (−2)	9.4069 (−2)	3.2708	2.8494
3.75				3.2512	2.8022
4.00	+1.6740 (−2)	6.5747 (−2)	7.7488 (−2)	3.2336	2.7693
4.25				3.2182	2.7509
4.50		6.0007 (−2)	7.3097 (−2)	3.2047	2.7456
4.75				3.1928	2.7511
5.00	+6.2074 (−3)	5.8604 (−2)	7.1946 (−2)	3.1821	2.7644
6.00	+3.2278 (−3)	5.8566 (−2)	6.9772 (−2)	3.1459	2.8468
7.00	+1.6052 (−3)	5.8862 (−2)	6.6618 (−2)	3.1193	2.9230
8.00	+7.2806 (−4)	5.9023 (−2)	6.3866 (−2)	3.1044	2.9836
9.00	+3.0329 (−4)	5.9098 (−2)	6.1945 (−2)	3.0986	3.0284
10.0	+1.1553 (−4)	5.9135 (−2)	6.0740 (−2)	3.0974	3.0587
11.0	+3.9288 (−5)	5.9152 (−2)	6.0740 (−2)		
12.0	+1.0491 (−5)	5.9161 (−2)	5.9627 (−2)	3.0985	3.0891
13.0	+8.4492 (−7)	5.9166 (−2)	5.9407 (−2)		
13.5	−9.3212 (−7)				
14.0	−1.7470 (−6)	5.9169 (−2)	5.9290 (−2)	3.0992	3.0986
14.5	−2.0257 (−6)				
15.0	−2.0187 (−6)		5.9229 (−2)		
15.5	−1.8903 (−6)				
16.0	−1.6909 (−6)	5.9171 (−2)	5.9199 (−2)	3.0995	3.1006
17.0	−1.2756 (−6)		5.9184 (−2)		
18.0	−9.3220 (−7)	5.9172 (−2)	5.9177 (−2)	3.0996	3.1008
19.0	−6.7548 (−7)		5.9174 (−2)		
20.0	−4.9290 (−7)	5.9173 (−2)	5.9173 (−2)	3.0997	3.1006
22.0	−2.7110 (−7)				3.1005
24.0	−1.5754 (−7)			3.0998	3.1004
26.0	−9.6299 (−8)				
28.0	−6.1414 (−8)			3.0999	3.1003
30.0	−4.0662 (−8)			3.1000	3.1002

$b = +1.66$ for the Σ-Σ transitions. The constructed curves in this way are shown in Fig. 3. We finally list in Table III some data points we have generated for both the interatomic KHe potentials and the corresponding $A \leftarrow X$ and $B \leftarrow X$ transition dipole moments. More data points can be provided by the authors upon request.

IV. POTENTIAL AND DIPOLE-MOMENT ASSESSMENTS

Once the constructions of the KHe potential energies and transition dipole moments have been fulfilled, it is appropriate and commendable to ensure their consistency and reliability.

A. Diffusion coefficient

To assess the accuracy of the interatomic potentials, we suggest calculating the temperature-dependent diffusion coefficient $\mathcal{D}$ of potassium atoms in a helium gas which is known to be very sensitive to the interatomic potential of the KHe molecule [44]. In the framework of the transport theory of *dilute* gases [45], the diffusion coefficient $\mathcal{D}$ is formulated as

$$\mathcal{D}(T) = \frac{3}{16n}\sqrt{\frac{2\pi k_B T}{\mu}}\frac{1}{\overline{\sigma}}, \tag{6}$$

where n is the number density of the perturber gas and $\overline{\sigma}$ is the average diffusion cross section defined by the integral

$$\overline{\sigma} = \frac{1}{2}\int_0^\infty x^2\sigma(x)\exp(-x)dx. \tag{7}$$

The ratio $x = E/(k_B T)$ is linked to the relative energy E and $\sigma(x)$ represents the cross section effective in diffusion given by

$$\sigma(x) = \frac{4\pi}{k^2}\sum_{l=0}^{\infty}(l+1)\sin^2(\eta_{l+1} - \eta_l), \tag{8}$$

TABLE IV. Diffusion coefficient $\mathcal{D}$, in cm^2/s, at pressure $p =$ 760 torr for the ground $X\,^2\Sigma^+$ state of KHe.

T(K)	This work	Ref. [46]
70	0.027	0.027
200	0.176	0.174
300	0.374	0.369
400	0.644	0.638
500	0.989	0.984
600	1.409	1.407
800	2.476	2.487
1000	3.841	3.906
1300	6.430	6.637
1600	9.637	10.134
1700	10.838	11.410
2000	14.820	15.897
3000	32.062	35.775

where $k = \sqrt{2\mu E/\hbar^2}$ is the wave number and η_l is the phase shift obtained by solving the radial wave equation (3) and forcing the wave function $\psi(R)$ to behave asymptotically like

$$\psi(R) \sim \sin\left(kR - \tfrac{1}{2}l\pi + \eta_l\right). \tag{9}$$

For the case of the first-excited molecular states, the coefficient of diffusion is evaluated by using the *average* diffusion cross section for the $A\,^2\Pi$ and $B\,^2\Sigma^+$ states; namely,

$$\overline{\sigma}_{\rm av} = \tfrac{2}{3}\overline{\sigma}_A + \tfrac{1}{3}\overline{\sigma}_B. \tag{10}$$

The diffusion cross sections of potassium for the ground $X\,^2\Sigma^+$ state and the excited $A\,^2\Pi$ and $B\,^2\Sigma^+$ states calculated from Eq. (8) are shown in Fig. 4. For the ground $X\,^2\Sigma^+$ state, the diffusion cross section passes through a minimum around $E = 1.66 \times 10^{-7}$, increases to a maximum at $E = 5.70 \times 10^{-7}$ and then decreases regularly. For the excited state $A\,^2\Pi$, the diffusion cross section shows a peak at the energy position $E = 1.72 \times 10^{-6}$ resulting from the shape resonance of the f wave, while the oscillations at higher energies arise from partial waves of higher orders. The diffusion cross section of the $B\,^2\Sigma^+$ state increases towards the maximum

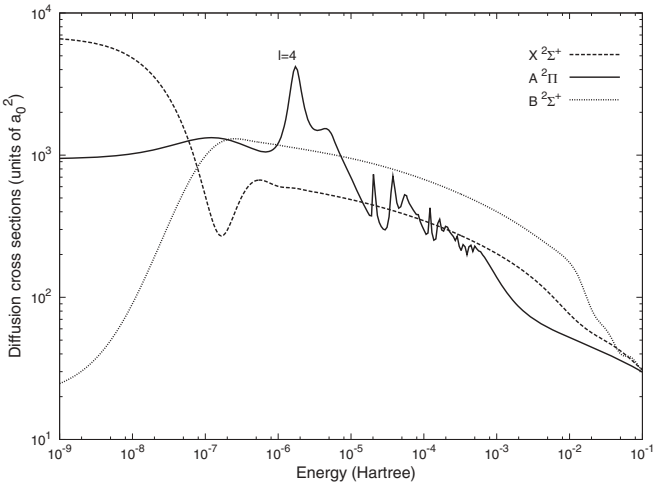

FIG. 4. Diffusion cross sections of the ground ($X\,^2\Sigma^+$) and excited ($A\,^2\Pi$ and $B\,^2\Sigma^+$) states of KHe.

in the vicinity of $E = 2.56 \times 10^{-7}$ then decreases gradually at higher energies.

The potassium diffusion coefficients at temperatures between 70 and 3000 K, computed with Eq. (6) at gas pressure $p = 760$ torr, are listed in Table IV for the X state and in Table V for the A and B states. A good concordance is found with previous calculations performed by Parkhomenko [46] over the same range of temperatures. Figure 5 displays, at the given pressure, the potassium diffusion coefficients of the ground X state in the temperature interval 600–1000 K. The results are compared with the measurements of Ivanovskiy *et al.* [47]. As reported by Redko and Kosinar [48], the experimental data are in many cases in error by not more than 15%. We have thus calculated the error bars and plotted them with the corresponding data. A good agreement can be observed. We have besides presented in the same figure, at the same pressure and over the same range of temperatures, the diffusion coefficients of potassium relative to the excited A and B states, as well as the average value computed from equation (6) using the relationship (10). To our knowledge, there are unfortunately no *experimental* values for these states to compare with.

TABLE V. Diffusion coefficients $\mathcal{D}$, in cm^2/s, at pressure $p = 760$ torr for the excited $A\,^2\Pi$ and $B\,^2\Sigma^+$ states of KHe.

Temperature	$A\,^2\Pi$		$B\,^2\Sigma^+$		Average	
T(K)	This work	Ref. [46]	This work	Ref. [46]	This work	Ref. [46]
70	0.032	0.021	0.014	0.013	0.022	0.018
200	0.278	0.208	0.088	0.083	0.162	0.138
300	0.637	0.514	0.184	0.174	0.350	0.311
400	1.122	0.961	0.312	0.297	0.601	0.550
500	1.719	1.539	0.472	0.453	0.914	0.855
600	2.415	2.236	0.665	0.645	1.287	1.227
800	4.083	4.149	1.160	1.142	2.219	2.210
1000	6.086	6.086	1.816	1.815	3.412	3.410
1300	9.671	9.896	3.145	3.195	5.717	5.824
1600	13.906	14.477	4.941	5.090	8.665	8.966
1700	15.456	16.170	5.652	5.841	9.793	10.174
2000	20.508	21.788	8.140	8.513	13.613	14.336
3000	41.558	44.719	20.596	22.015	31.030	33.279

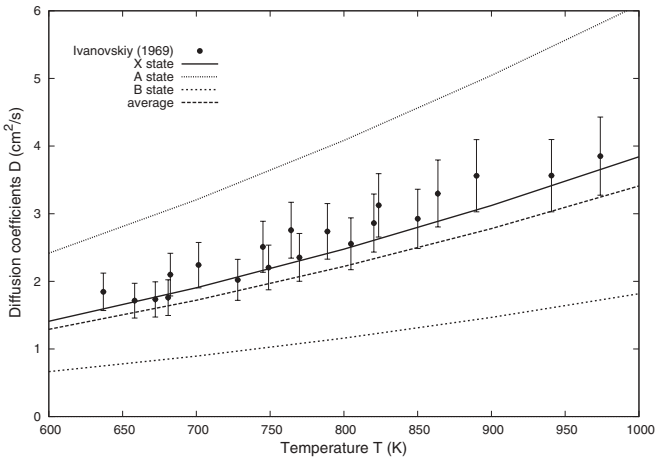

FIG. 5. Temperature dependence of potassium diffusion coefficients $\mathcal{D}$ at pressure $p = 760$ torr. The solid and dotted lines give the computed values. The points represent the experimental data from Ivanovskiy *et al.* [47].

B. Radiative lifetime

To further establish the correctness of our potential curves and transition dipole moments, we have specifically calculated the radiative lifetimes of the rovibrational levels of the $A\,^2\Pi$ states of the excited KHe dimer. In quantum theory, the lifetime τ of a given (v', J', Λ') level verifies the relationship [6,7]

$$\frac{1}{\tau} = \frac{64\pi^4}{3hc^3} g \int_0^\infty \nu^3 |\langle \psi_{v'J'\Lambda'} | D(R) | \psi_{\epsilon'' J'\Lambda''} \rangle|^2 d\epsilon'', \qquad (11)$$

with $g = 1$ being the electronic degeneracy relative to the A-X transition. The obtained results for the $A\,^2\Pi$-state levels are listed in Table VI. From this table, the lifetime of the last level near the dissociation limit should match the value for the state $4p\,^2P$ of atomic potassium. In such a case, our calculation yields the lifetime value 26.74 ± 0.02 ns. This value is largely comfortable with those measured experimentally, 26.56 ns by Volz and Schromanzer [42], 26.45 ± 0.05 ns by Wang *et al.* [43], 27.0 ± 0.1 ns by Reho *et al.* [35], and 26.51 ± 0.03 ns by Falke *et al.* [49], or determined theoretically, 26.27 ns by Froese-Fischer [50], 27.38 ns by Safranova *et al.* [51], and 26.2 ns for the rotationless KHe ($v = 3$, $J = 0$) state by Zhu *et al.* [5]. Moreover, Serrão [52] has recently gathered some potassium lifetime results, which all agree with the NIST recommended weighted value 26.06 ns [53].

TABLE VI. Radiative lifetimes τ (in ns) of the rovibrational levels of the $A\,^2\Pi$ state. The first row contains our calculated lifetimes generated with $D_\infty = 2.92$ a.u. The second row gives the results from Ref. [5].

J	$v=0$	$v=1$	$v=2$	$v=3$	$v=4$	$v=5$
0	32.6	30.3	28.2	26.7		
	28.3	26.6	25.2	26.2	79.8	30.0
5	32.5	30.1	27.9			
	28.2	26.4	25.1	27.1	106.9	
10	32.1	29.5				
	27.9	26.1	24.6			
15	31.3					
	27.4					

V. RESULTS AND DISCUSSION

Once the initial assessments of the potentials and dipole moments, both requested for the computation of precise photoabsorption coefficients and for the analysis of their behavior with temperature, have been achieved, we give hereafter some computational details and mention the main results and remarks arising from the KHe calculations.

The normalized wave functions appearing in Eqs. (1) and (2) are obtained by solving numerically the radial wave equation (3) with the Numerov algorithm [54]. For the *free-free* integral in Eq. (1), we used the Gauss-Laguerre quadrature with 100 weighted points [55] and, to avoid the numerical problem arising from the divergence of the matrix elements in Eq. (1), we have adopted the method already described in Ref. [6]. The reduced absorption coefficients are mainly output by including all the *bound* and *quasibound* levels. To generate the photoabsorption profile, we have carried out calculations, for all temperatures, with a frequency step size $\Delta\nu = 10\ \text{cm}^{-1}$ taking the rotational quantum number J no more than $J_{\max} = 25$ and $J_{\max} = 250$ for the *free-bound* and *free-free* transitions, respectively.

The reduced absorption coefficients, around the K($4p \leftarrow 4s$) resonance line $\lambda_0 = 770$ nm, are determined in the far wings by transitions from the ground to the excited KHe states. Since the $X\,^2\Sigma^+$ and $B\,^2\Sigma^+$ electronic states are repulsive and the $A\,^2\Pi$ state possesses a shallow potential well, the absorption coefficients are subsequently the contribution of the *free-free* $A \leftarrow X$, $B \leftarrow X$ and *free-bound* $A \leftarrow X$ transitions. As can be remarked in Fig. 6, which presents the partial reduced absorption coefficients, the shape of the KHe spectra emerges basically from the $B \leftarrow X$ transitions in the *blue* wings and from the $A \leftarrow X$ transitions in the *red* wings. In other words, the blue wings result from *free-free* transitions, whereas the red wings arise from the sum of *free-bound* and *free-free* transitions. Furthermore, in the red wings, the *free-free* transitions are dominant compared with the *free-bound* transitions for all considered temperatures. Hence, the photoabsorption spectra of the KHe molecule is dominated by the *free-free* transitions for all temperatures.

Figure 7 shows our theoretical and full *quantum-mechanical* spectra at different temperatures; namely, $T = 500$, 1000, 2000, and 3000 K, in the wavelength interval going from 650 to 950 nm. It is easy to see that, from the line center, both wings display at one specific temperature a rapidly decreasing spectrum, but the reduced absorption coefficient increases in magnitude with increasing temperatures. At some position in the far-blue wings, the spectra exhibit around the wavelength 693.0 ± 0.5 nm a satellite for all the temperatures cited above. This leads us to conclude that the satellite starts to grow at $T \lesssim 500$ K.

On the other hand, we have at our disposal a few published theoretical works. The first one deals with the photoabsorption spectra calculations performed by Allard *et al.* [1] in the framework of the unified approach based on the KHe potentials and dipole moments produced by Pascale [38]. Allard *et al.* have found at the same temperatures a blue-wing satellite

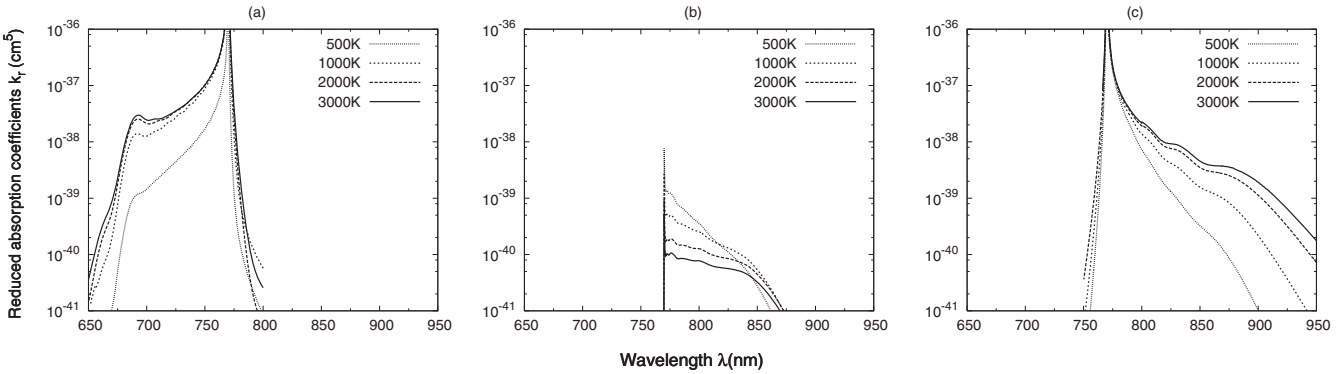

FIG. 6. Partial reduced absorption coefficients presented respectively from left to right at temperatures 500, 1000, 2000, and 3000 K. Panel (a) represents the *free-free* $X\,^2\Sigma^+$-$B\,^2\Sigma^+$ transitions and panels (b) and (c) represent the *free-bound* and *free-free* $X\,^2\Sigma^+$-$A\,^2\Pi$ transitions, respectively.

located around the wavelength of 690 nm. The second work treats the *emission* and *absorption* profiles, which Zhu, Babb, and Dalgarno [5] have recently generated, using a quantum-mechanical approach. These authors, by adopting the interatomic potential and dipole moment curves computed by Santra and Kirby [40], found a satellite near the wavelength 708 nm for $T \simeq 1000$–3000 K. Besides, using the quasistatic theory of absorption spectra, fully described in Szudy and Baylis [56], Burrows and Volobuyev [12] arrived in their calculations to the KHe satellite features close to the wavelength position of 690 nm and reported, from Ch'en and Wilson [57], the measurements of the violet band separation for the satellite features on the KHe blue wings to be 838 ± 5 cm^{-1}, which translate into the satellite position around 720 nm [12]. Also, in their experimental work, held at temperature of 673 K, Vdović *et al.* [58] could not observe the blue satellite, but nevertheless succeeded to find it near the blue-wing position 690 nm from classical calculations. In addition, we have an experimental spectrum measured by Shindo and Yoshino [19,20] at the temperature 950 K, with the potassium density being around 6×10^{15} cm^{-3} and the He gas pressure between 170 and 700 torr. In Fig. 8, we compare our reduced absorption coefficient calculated at the temperature of 1000 K with these measured data. In the same Fig. 8, we also plotted the spectra at 1000 K of Allard *et al.* [1] and Zhu *et al.* [5]. All the theoretical spectra have been shifted to the experimental results. One may easily see that these spectra have the same general shape and, mainly, that the satellite peaks occur in the same wing, around close positions. This confirms that our results are in good agreement with previous calculations and measurements and demonstrates, in particular, the sensitivity of the pressure-broadening calculations on the accuracy and quality of the potentials and transition dipole moments.

VI. CONCLUSION

We have performed in this work quantum-mechanical calculations related to the KHe absorption profile in the wavelength domain of 650–950 nm and in the temperature domain of 500–3000 K. For this purpose, we have computed accurate ground ($X\,^2\Sigma^+$) and excited ($A\,^2\Pi$ and $B\,^2\Sigma^+$) interatomic potentials and transition dipole moments using the *ab initio* SA-CASSCF and MRCI methods, including the Davidson and BSSE corrections. The accuracy of the constructed potentials and dipole moments has been tested by

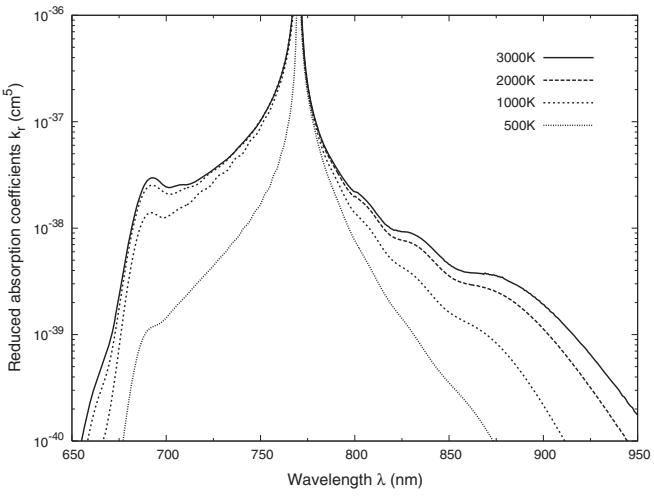

FIG. 7. Representation of the full quantum-mechanical reduced absorption coefficients at different temperatures.

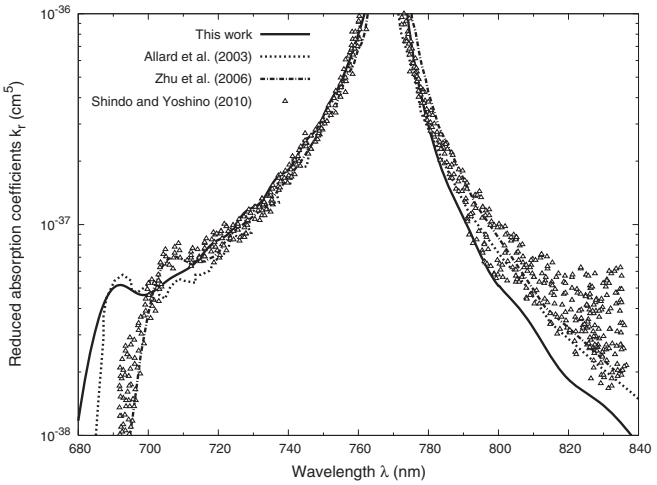

FIG. 8. Theoretical reduced absorption coefficients computed at 1000 K compared with those measured at 950 K by Shindo and Yoshino [19,20].

determining the diffusion coefficients at various temperatures and the radiative lifetimes of the $A\,^2\Pi$ rovibrational levels. We have then analyzed the temperature-dependant absorption coefficients and located a blue satellite around 693 nm, which arises from the *free-free*$B \leftarrow X$ transitions. We have also compared our calculated spectra at 1000 K with other theoretical and experimental results.

ACKNOWLEDGMENTS

A part of this work has been realized at the LASIM, Claude Bernard University, Lyon 1, France. The Algerian authors (H.B., K.A., and M.B.) are very grateful to LASIM and to the Algerian *Ministry of Higher Education and Scientific Research* for support.

[1] N. F. Allard, F. Allard, P. H. Hauschildt, J. F. Kielkopf, and L. Machin, Astron. Astrophys. **411**, L473 (2003).

[2] N. F. Allard, F. Allard, and J. F. Kielkopf, Astron. Astrophys. **440**, 1195 (2005).

[3] N. F. Allard and F. Spiegelman, Astron. Astrophys. **452**, 351 (2006).

[4] C. Zhu, J. F. Babb, and A. Dalgarno, Phys. Rev. A **71**, 052710 (2005).

[5] C. Zhu, J. F. Babb, and A. Dalgarno, Phys. Rev. A **73**, 012506 (2006).

[6] K. Alioua and M. Bouledroua, Phys. Rev. A **74**, 032711 (2006).

[7] K. Alioua, M. Bouledroua, A. R. Allouche, and M. Aubert-Frécon, J. Phys. B **41**, 175102 (2008).

[8] F. Shindo, J. F. Babb, K. Kirby, and K. Yoshino, J. Phys. B **40**, 2841 (2007).

[9] M. Shurgalin, W. H. Parkinson, K. Yoshino, C. Schoene, and W. P. Lapatovitch, Meas. Sci. Technol. **11**, 730 (2000).

[10] H.-K. Chung, M. Shurgalin, and J. F. Babb, AIP Conf. Proc. **645**, 211 (2002).

[11] A. Burrows, in *Brown Dwarfs*, Proceedings of IAU Symposium #211, held 20–24 May 2002 at University of Hawaii, Honolulu, Hawaii, edited by E. Martín (Astronomical Society of the Pacific, San Francisco, 2003).

[12] A. Burrows and M. Volobuyev, Astrophys. J. **583**, 985 (2003).

[13] A. Burrows, Nature (London) **433**, 261 (2005).

[14] C. Sharp and A. Burrows, Astrophys. J. Suppl. Ser. **168**, 140 (2007).

[15] A. Chattopadhyay, J. Phys. B **44**, 165101 (2011).

[16] A. Chattopadhyay, J. Phys. B **45**, 035101 (2012).

[17] J. D. Readle, C. J. Wagner, J. T. Verdeyen, D. L. Carroll, and J. G. Eden, Electron. Lett. **44**, 1466 (2008).

[18] J. D. Readle, C. J. Wagner, J. T. Verdeyen, T. M. Spinka, D. L. Carroll, and J. G. Eden, Appl. Phys. Lett. **94**, 251112 (2009).

[19] J. Babb, *Pressure Broadening of Alkali-Metal Resonance Lines in the Presence of Helium or Molecular Hydrogen*, presented at the One-Day Symposium on Laboratory Astrophysics at the CfA, September 20, 2010, Cambridge, MA http://www.cfa.harvard.edu/events/2010/labastro/.

[20] F. Shindo and K. Yoshino, cited in Ref. [19].

[21] H. J. Werner and P. J. Knowles, J. Chem. Phys. **89**, 5803 (1988).

[22] P. J. Knowles and H. J. Werner, Chem. Phys. Lett. **145**, 514 (1988).

[23] H. J. Werner and P. J. Knowles, J. Chem. Phys. **82**, 5053 (1985).

[24] P. J. Knowles and H. J. Werner, Chem. Phys. Lett. **115**, 259 (1985).

[25] E. R. Davidson and D. W. Silver, Chem. Phys. Lett. **53**, 403 (1977).

[26] S. F. Boys and F. Bernardi, Mol. Phys. **19**, 553 (1970).

[27] J.-P. Blaudeau, M. P. McGrath, L. A. Curtiss, and L. Radom, J. Chem. Phys. **107**, 5016 (1997).

[28] D. E. Woon and T. H. Dunning Jr., J. Chem. Phys. **100**, 2975 (1994).

[29] H.-J. Werner, P. J. Knowles, R. Lindh, F. R. Manby, M. Schütz, P. Celani, T. Korona, G. Rauhut, R. D. Amos, A. Bernhardsson, A. Berning, D. L. Cooper, M. J. O. Deegan, A. J. Dobbyn, F. Eckert, C. Hampel, G. Hetzer, A. W. Lloyd, S. J. McNicholas, W. Meyer, M. E. Mura, A. Nicklass, P. Palmieri, R. Pitzer, U. Schumann, H. Stoll, A. J. Stone, R. Tarroni, and T. Thorsteinsson, MOLPRO, version 2002.6, a package of *ab initio* programs.

[30] J. Mitroy and M. W. J. Bromley, Phys. Rev. A **68**, 062710 (2003).

[31] J. Mitroy and M. W. J. Bromley, Phys. Rev. A **71**, 019903(E) (2005).

[32] J.-Y. Zhang and J. Mitroy, Phys. Rev. A **76**, 022705 (2007).

[33] A. Nakayama and K. Yamashita, J. Chem. Phys. **114**, 780 (2001).

[34] S. H. Patil, J. Chem. Phys. **94**, 8089 (1991).

[35] J. Reho, J. Higgins, K. K. Lehmann, and G. Scoles, J. Chem. Phys. **113**, 9694 (2000).

[36] F. Masnou-Seeuws, M. Philippe, and P. Valiron, Phys. Rev. Lett. **41**, 395 (1978).

[37] F. Masnou-Seeuws, J. Phys. B **15**, 883 (1982).

[38] J. Pascale, Phys. Rev. A **28**, 632 (1983).

[39] M. Zbiri and C. Daul, J. Chem. Phys. **121**, 11625 (2004).

[40] R. Santra and K. Kirby, J. Chem. Phys. **123**, 214309 (2005).

[41] X. Chu and A. Dalgarno, Phys. Rev. A **66**, 024701 (2002).

[42] U. Volz and H. Schmoranzer, Phys. Scr. **65**, 48 (1996).

[43] H. Wang, J. Li, X. T. Wang, C. J. Williams, P. L. Gould, and W. C. Stwalley, Phys. Rev. A **55**, R1569 (1997).

[44] J. O. Hirschfelder, C. F. Curtis, and R. B. Bird, *Molecular Theory of Gases and Liquids* (Wiley and Sons, New York, 1964).

[45] A. Dalgarno, in *Atomic and Molecular Processes*, edited by D. R. Bates (Academic Press, New York, 1962).

[46] A. I. Parkhomenko, Opt. Spectrosc. **67**, 14 (1989).

[47] M. N. Ivanovskiy, V. P. Sorokin, V. I. Subbotin, and B. A. Chulkov, Teplofiz. Vys. Temp. **7**, 479 (1969).

[48] T. P. Redko and I. Kosinar, Czech. J. Phys. B **30**, 1293 (1980).

[49] S. Falke, I. Sherstov, E. Tiemann, and C. Lisdat, J. Chem. Phys. **125**, 224303 (2006).

[50] C. Froese-Fisher, Nucl. Instrum. Methods Phys. Res., Sect. B **31**, 265 (1988).

[51] M. S. Safronova, W. R. Johnson, and A. Derevianko, Phys. Rev. A **60**, 4476 (1999).

[52] J. M. P. Serrão, J. Quantum Spectr. Rad. Transfer **109**, 453 (2008).

[53] A. Kramida, Yu. Ralchenko, J. Reader, and NIST ASD Team. *NIST Atomic Spectra Database* (ver. 5.0). Available at http://physics.nist.gov/asd National Institute of Standards and Technology, Gaithersburg, MD (2012).

[54] B. Numerov, Publ. Observ. Central Astrophys. Russ. **2**, 188 (1933).

[55] W. H. Press, B. P. Flannery, S. A. Teukolsky, and W. T. Vetterling, *Numerical Recipes. The Art of Scientific Computing* (Cambridge University Press, New York, 1987).

[56] J. Szudy and W. Baylis, Phys. Rep. **266**, 127 (1996).

[57] S. Y. Ch'en and R. A. Wilson, Physica **27**, 497 (1961).

[58] S. Vdović, R. Beuc, D. Aumiler, T. Ban, and G. Pichler, J. Phys. B **38**, 3107 (2005).